Chiral Discrimination in the Dissociation of the Intermolecular Excimer of *N*-Acetyl-1-pyrenylalanine Methyl Ester

F. López-Arbeloa,[†] R. Goedeweeck,[†] F. Ruttens,[†] F. C. De Schryver,*[†] and M. Sisido[‡]

Contribution from the Laboratory for Spectroscopy and Molecular Dynamics, Katholieke Universiteit Leuven, B-3030 Heverlee-Leuven, Belgium, and the Research Center for Medical Polymers and Biomaterials, Kyoto University, Kyoto 606, Japan. *Received October 16, 1986*

Abstract: Intermolecular excimer formation of the racemic mixture and the optically pure enantiomer of *N*-acetyl-1-pyrenylalanine methyl ester is studied by stationary (fluorescence spectroscopy) and transient techniques (time-correlated single-photon counting). In this study, solvents with different tendency to interact by hydrogen bonding with the peptide function are used. Although no important differences in the rate constant of excimer formation between the racemic mixture and the optically pure enantiomer are observed, a lower rate constant for the dissociation from the D–L excimer to the locally excited state than from the L–L excimer is obtained at room temperature. The D–L excimer is characterized by a stabilization enthaply that is 3 kcal/mol larger than that of the L–L excimer in inert solvents, which can be explained by hydrogen bonding between the amino acid functions in the excimer state. Destabilization of the L–L excimer with respect to the D–L excimer in hydrogen-accepting solvents is due to the larger steric hindrance between the solvated amide groups in the L–L excimer than in the D–L excimer.

Differences in the photophysical properties between a racemic and the corresponding optically pure enantiomer have been observed for some time.[1-6] Chiral discrimination in excimer formation is due to a difference in the intermolecular interaction probability of homotactic and heterotactic pairs or to a different overlap and formation rate of the intramolecular excimer of diastereoisomeric bichromophores.[7,8]

Fluorescence studies of the quenching processes of a chromophore[9] with chiral substituents provide information on the chiral discrimination, e.g., fluorescence quenching of (*R*)-(−)-1,1′-binaphthyl by chiral amines,[10,11] the intermolecular excimer formation of pyrenyl derivatives,[12-15] and the asymmetric photoreaction in the tris(bipyridyl)ruthenium(II) complex.[16]

Important differences in the emission properties of the erythro and threo diastereoisomer of bis(1-pyrenyl)alanines[17-19] and of 1-pyrenylalanine-1-methylthryptophan[20,21] dipeptides have been measured in our laboratory. These differences results from the fact that the conformational distribution of the peptide chain related to both the solvent and the chirality of the chain has a determining influence on the process of excimer formation.

In order to study the possible chiral discrimination in the intermolecular excimer formation of α-amino acids, racemic *N*-acetyl-1-pyrenylalanine methyl ester (A1PME) was synthesized and resolved in its two optical enantiomers (D- and L-A1PME).

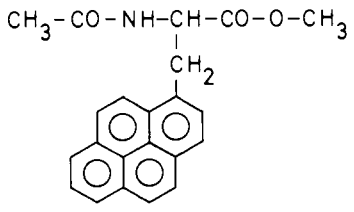

The intermolecular excimer formation of the racemic mixture (DL-A1PME) and the optically pure enantiomer (L-A1PME) is studied in three solvents with different tendency to interact by hydrogen bonding with the peptide function: acetonitrile and toluene as inert solvents with different polarity and *N*,*N*′-dimethylformamide (DMF), which is a hydrogen-accepting solvent. The thermodynamic parameters of the excimer formation and dissociation can be calculated from a combined fluorescence study under stationary and nonstationary conditions of excitation as a function of temperature.

Synthesis and Methods

N-Acetyl-1-pyrenylalanine methyl ester was synthesized and resolved following the procedure developed by Egusa et al[14] (Scheme I).

2-Phenyl-4-(1-pyrenylmethylene)-5-oxazolone (**2**)[22] was obtained by heating (95–100 °C) 1-pyrenaldehyde (**1**) with hippuric acid and sodium acetate in acetic anhydride. The red oxazolone **2** was gradually added with stirring to a solution of sodium–ethanol/benzene (3:1). The yellow ethyl 3-(1-pyrenyl)-2-benzamidopropenate (**3**) was collected and hydrogenated to *N*-benzoyl-1-pyrenylalanine ethyl ester (**4**) by palladium carbon in ethanol/ethyl acetate (1:1) at room temperature. **4** was hydrolyzed to *N*-benzoyl-1-pyrenylalanine (**5**) by heating at 50–60 °C in ethanol with aqueous sodium hydroxide.

Racemic **5** was dissolved in ethanol by heating and adding (+)-1-phenylethylamine. After 2 days at −40 °C a precipitate, the diastereoisomeric salt [L-(**5**)---(+)-amine], was obtained, recrystallized twice with ethanol, and hydrolyzed to the corresponding L-(**5**) with aqueous hydrochloric acid. All the filtrates (rich in [D-(**5**)---(+)-amine] salt) was acidified with aqueous hydrochloric acid, and D-(**5**) was obtained, which was again resolved with the corresponding (−)-1-phenylethylamine by the same procedure. The precipitation of each diastereoisomer was not quantitative, and consecutive resolutions were performed by successive additions of (+)- and (−)-amine to the rich L- and D-(**5**), respectively, until an appreciable amount of L- and D-(**5**) was obtained. The optical purity of the enantiomers was determined by measuring the optical rotation angle: values of $[\alpha]^{25}_{D}$ = −221.0 and 207.6 for L- and D-(**5**), respectively, (5 mg/mL in dimethylformamide) were obtained. From

[†] Katholieke Universiteit Leuven.
[‡] Kyoto University.

(1) Hayward, L. D.; Totty, R. N. *Can. J. Chem.* **1971**, *49*, 624.
(2) Craig, D. P.; Mellor, D. P. *Top. Curr. Chem.* **1976**, *63*, 1.
(3) Mason, S. F. *Annu. Rep. Prog. Chem., Sect. A: Phys. Inorg. Chem.* **1976**, *73*, 53.
(4) Steinberg, I. Z. *Annu. Rev. Biophys. Bioeng.* **1978**, *7*, 113.
(5) Kuroda, R.; Mason, S. F.; Rodger, C. D.; Seal, R. H. *Chem. Phys. Lett.* **1978**, *57*, 1.
(6) Rau, H. *Chem. Rev.* **1983**, *83*, 535.
(7) Collart, P.; Demeyer, K.; Toppet, S.; De Schryver, F. C. *Macromolecules* **1983**, *16*, 1390.
(8) Vandendriessche, J.; Palmans, P.; Toppet, S.; Boens, N.; De Schryver, F. C.; Masuhara, H. *J. Am. Chem. Soc.* **1984**, *106*, 8057.
(9) Birks, J. B. *Photophysics of Aromatic Molecules*; Interscience: New York, 1973.
(10) Irie, M.; Yorozu, T.; Hayashi, K. *J. Am. Chem. Soc.* **1978**, *100*, 2236.
(11) Yorozu, T.; Hayashi, K.; Irie, M. *J. Am. Chem. Soc.* **1981**, *103*, 5488.
(12) Tran, C. D.; Fendler, J. H. *J. Am. Chem. Soc.* **1980**, *102*, 2923.
(13) Brittain, H.; Ambrozich, D. L.; Saburi, N.; Fendler, J. H. *J. Am. Chem. Soc.* **1980**, *102*, 6372.
(14) Egusa, S.; Sisido, M.; Imanishi, Y. *Macromolecules* **1985**, *18*, 882.
(15) Kano, K.; Matsumoto, H.; Hashimoto, S.; Sisido, M.; Imanishi, Y. *J. Am. Chem. Soc.* **1985**, *107*, 6117.
(16) Rau, H.; Ratz, R. *Angew. Chem.* **1983**, *95*, 552.
(17) Goedeweeck, R.; De Schryver, F. C. *Photochem. Photobiol.* **1984**, *39*, 515.
(18) Goedeweeck, R.; Van der Auweraer, M.; De Schryver, F. C. *J. Am. Chem. Soc.* **1985**, *107*, 2334.
(19) Goedeweeck, R.; Ruttens, F.; Lopez-Arbeloa, F.; De Schryver, F. C., submitted for publication.
(20) Ruttens, F.; Goedeweeck, R.; Lopez-Arbeloa, F.; De Schryver, F. C. *Photochem. Photobiol.* **1985**, *42*, 341.
(21) Ruttens, F.; Goedeweeck, R.; Lopez-Arbeloa, F.; De Schryver, F. C., submitted for publication.
(22) Lettre, H.; Buchholz, K.; Fernholz, M. E. *Z. Phys. Chem. (Leipzig)* **1941**, *267*, 108.

0002-7863/87/1509-3068$01.50/0

Scheme I. Synthesis and Resolution of *N*-Acetyl-1-pyrenylalanine Methyl Ester

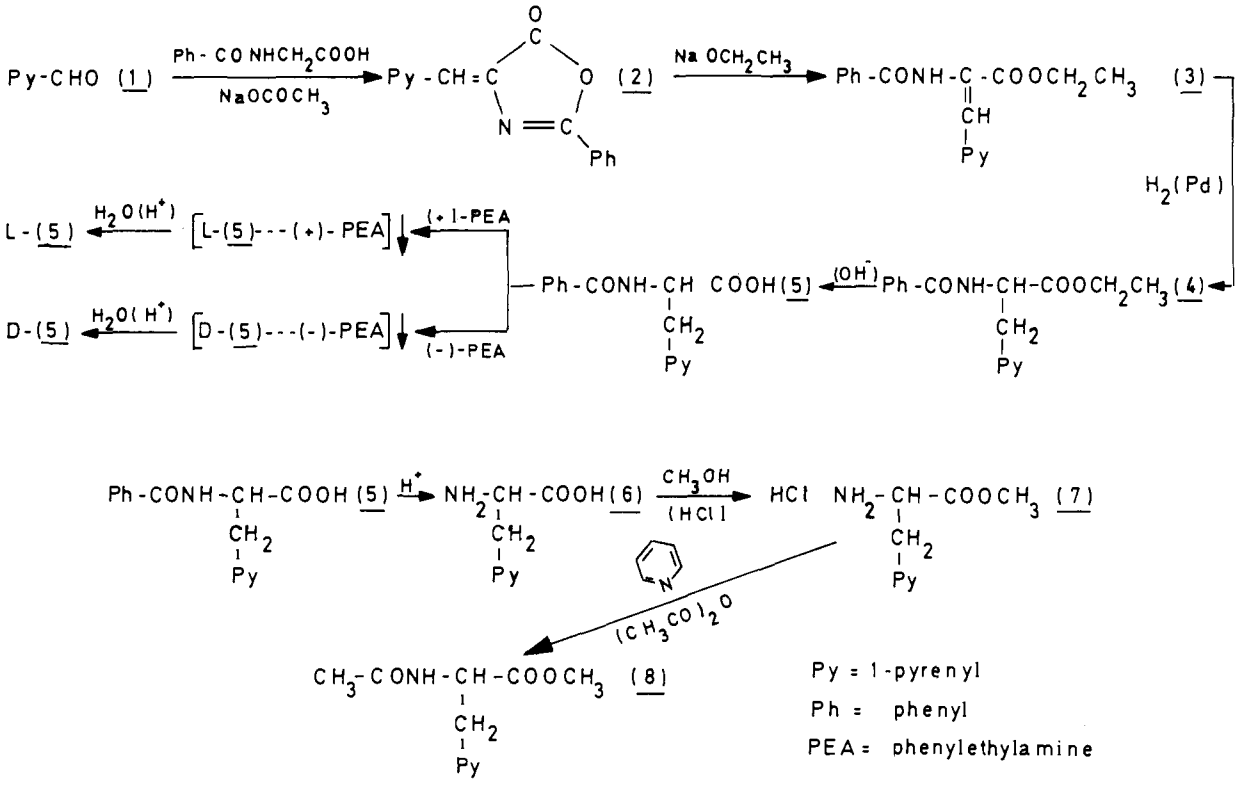

these values an optical purity of 97% and 95% for L- and D-(**5**), respectively, was calculated.

DL-, D-, and L-(**5**) were debenzoylated to 1-pyrenylalanine (**6**) by refluxing **5** in a mixture of acetic acid/hydrochloric acid (4:1), and the corresponding amino acids methyl ester hydrochloride **7** were obtained after refluxing **6** in methanol saturated with hydrochloric acid. The latter compounds were converted to *N*-acetyl-1-pyrenylalanine methyl ester (**8**) by acetic anhydride in the presence of pyridine. The optical purity of D- and L-(**8**) was controlled in ^1H NMR spectroscopy after adding 1.2 equiv of tris[3-((trifluoromethyl)hydroxymethylene)-*d*-camphorato]europium-(II) in $CDCl_3$. The signal of the methyl ester group of **8** was shifted to 5.3 ppm, and a single peak from D- and L-(**8**) was observed, indicating that the optical purity of both enantiomers has been maintained during the synthesis.

The racemic and optically pure *N*-acetyl-1-pyrenylalanine methyl ester (A1PME) were recrystallized from methanol and purified by column chromatography on silica gel with ethyl acetate as mobile phase. A last recrystallization was performed with *n*-hexane, and the compounds were dried in vacuo.

The intermolecular excimer formation of A1PME was studied in a concentration range from 1.0×10^{-4} up to 1.2×10^{-2} M (except in toluene where A1PME was only completely soluble up to a concentration of 3.2×10^{-3} M). All the solvents were spectroscopic grade and showed no emission in the wavelength region under study. All the measurements were performed with reference to a diluted solution of A1PME (10^{-6} M) unable to form a intermolecular excimer. All the solutions were degassed by the freezen–pump–thaw technique, and the emission intensities were measured in front-face mode in order to diminish reabsorption effects.

Absorption spectra were recorded on a Perkin-Elmer 550S spectrophotometer and fluorescence spectra on a SPEX Fluorolog. Sample thermostatization was realized with a methanol bath for low temperatures and a water bath for high temperatures. Fluorescence decay curves were measured by means of the time-correlated single-photon technique. Excitation was performed at 340 nm with a frequency-doubled, cavity-dumped DCM-dye laser synchronously pumped by a mode-locked argon laser.[23] All decay curves at high concentration were measured in a 1-mm cell oriented 45° with respect to the excitation and the analysis beam after thermostatization by a cold nitrogen flow for low temperatures and by a water bath for high temperatures. The goodness of fit of the calculated decay curves was controlled by the reduced χ^2, the ordinary runs (O.R.), and the Durbin–Watson (D.W.) statistical parameters.[24]

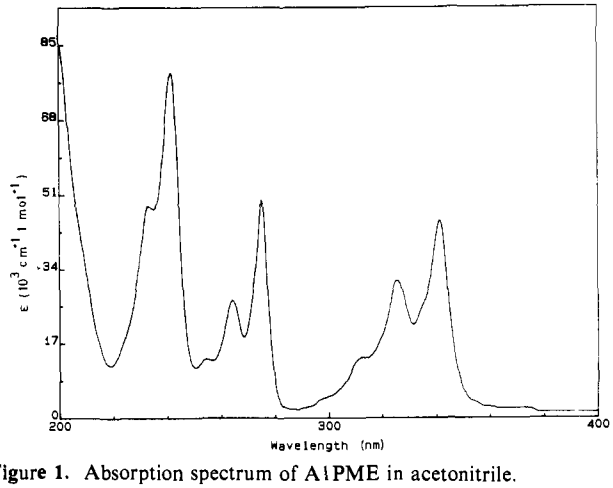

Figure 1. Absorption spectrum of A1PME in acetonitrile.

The change in the solvent volume with the temperature was taken into account by using the temperature variation of the solvent density. At all temperatures, the fluorescence spectra and decay curves were recorded twice for both concentrations 10^{-2} and 2×10^{-3} M. In general, the values of the rate constants were reproducible and remained constant with the concentration. The results listed in the tables are the average values of those four measurements, and the experimental error is included.

Results

Figure 1 shows the absorption spectrum of A1PME in a diluted solution in acetonitrile. The positions of the absorption maxima at 343 and 314 nm (^1L_a band) are identical with that of 1-methylpyrene (1MP) and show very low solvent dependence (in DMF a bathochromic shift of 2 nm is observed with respect to acetonitrile), but a larger molar extinction coefficient was calculated for A1PME (ϵ_{343}, 45 300 vs. 32 400 cm^{-1} mol^{-1}).[25] Pyrene has a molar extinction coefficient of 54 300 cm^{-1} mol^{-1} at the absorption maximum of the ^1L_a band.[26] Similar changes have

(23) Van den Zegel, M.; Boens, N.; De Schryver, F. C. *Biophys. Chem.* **1984**, *20*, 333.

(24) Boens, N.; Van den Zegel, M.; De Schryver, F. C. *Chem. Phys. Lett.* **1984**, *111*, 340.

(25) Baliah, V.; Pillay, K. *Indian J. Chem.* **1971**, *9*, 815.

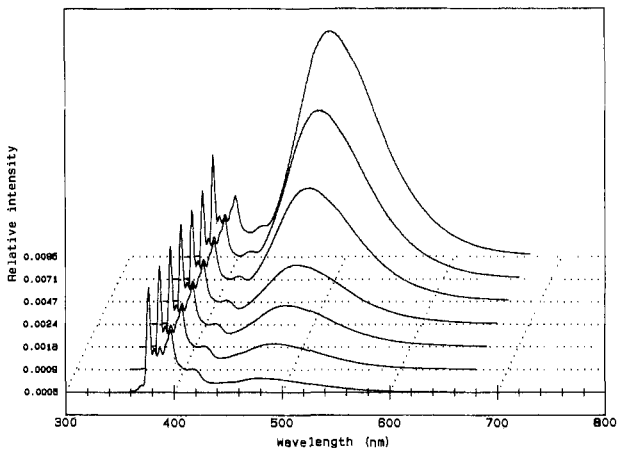

Figure 2. Fluorescence spectra of A1PME in acetonitrile at different concentrations (left edge) at room temperature, λ_{exc} = 343 nm.

been observed for the phenyl chromophore,[27] and they have been interpreted in terms of the inductive effect of the substitutent on the chromophore. The inductive effect of the amino acid chain in A1PME is diminished compared to the methyl substituent in 1MP due to the hetero atoms of the peptide function. Also the ^1L_b transition is influenced by this substitution as can be seen in the fluorescence lifetime in diluted solution, which equals 200–300 ns for A1PMe (depending on the solvent), intermediate between pyrene (300–400 ns)[28] and 1MP (150–250 ns).

No changes in the absorption spectrum of A1PME are observed when the concentration is increased up to 3.3×10^{-4} M (A_{343} = 1.5 in a 1-mm cell), indicating that no important interactions between the pyrenyl groups occur in the ground state. Appreciable excimer emission, however, is already observed at this concentration range. Excitation spectra are measured in order to verify the absence of ground-state pyrene–pyrene interactions at concentrations higher than 3.3×10^{-4} M. Despite some differences owing to the front-face mode, the excitation spectra of A1PME at high concentration (10^{-2} M) analyzed at 378 (locally excited state) and 490 nm (excimer emission region) are quite similar. In addition, transient fluorescence spectra at different delay times after excitation at high concentration of A1PME revealed no excimer emission at a delay time less than 1 ns. If ground-state interactions would occur in this concentration range, an excimer formed immediately after excitation should be expected. Therefore, it is concluded that no interaction between the pyrene groups in the ground state occurs, even at a concentration of 10^{-2} M.

On the contrary, the fluorescence spectra of A1PME shows a large concentration dependence (Figure 2). Besides the normal pyrenyl emission maxima (377 and 398 nm), a new broad and structureless emission band of the excimer appears when the concentration is increased. The maximum of the excimer band (obtained by subtracting the spectrum of a diluted solution after normalization of 398 nm) is determined at 485 nm in both DL- and L-A1PME and is independent of solvent polarity; only a small bathochromic shift of 2 nm in DMF with respect to acetonitrile and toluene is observed. No differences in the shape of the excimer band of A1PMe compared to 1MP are observed in the solvents studied.

The evolution of the ratio of the quantum yield of the excimer (ϕ_D) and the emission from the locally excited state (ϕ_M) with the concentration is shown in Figure 3 (as it is difficult to determine the total quantum yield of the spectrum recorded in

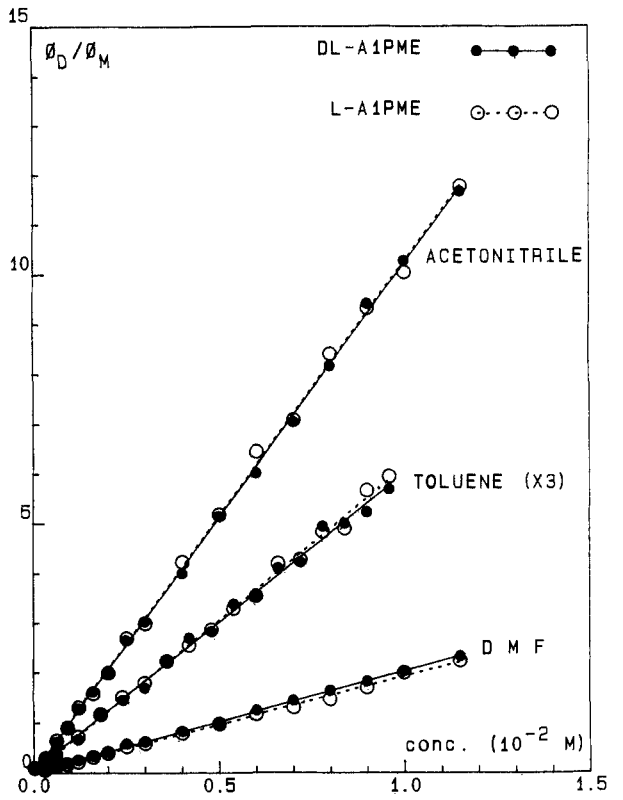

Figure 3. Ratio of the quantum yield of excimer emission (ϕ_D) and that of the locally excited state (ϕ_M) of racemic (DL-) and optically pure (L-) A1PME vs. the concentration at room temperature.

front-face mode, this ratio is calculated assuming that $\phi_D + \phi_M = 1$[10]). No deviation in the linear relationship of ϕ_D/ϕ_M vs. concentration is observed in the concentration range studied, suggesting that no ground-state aggregation between the peptide function of A1MPE occurs. Moreover, no evidence for intermolecular aggregation is observed in the NH stretching region of the infrared spectra of A1PME in chloroform. The slopes from Figure 3 are related to the rate constant of excimer formation (eq 1) according to the kinetic scheme developed by Birks,[9] where

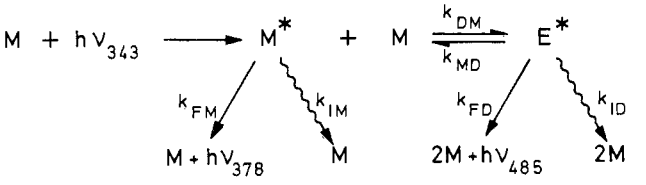

Birks scheme

$$\frac{\phi_D}{\phi_M} = \left(\frac{k_{FD}}{k_{FM}}\right)\left(\frac{k_{DM}}{k_{MD} + k_D}\right)[M] = K[M] \qquad (1)$$

k_{DM} and k_{MD} are the rate constants of excimer formation and dissociation from the excimer to the locally excited state, respectively, k_{FM} and k_{FD} are the rate constants of the radiative decay from the monomer and excimer, respectively, $k_D = k_{FD} + k_{ID}$, and $k_M = k_{FM} + k_{IM}$, where k_{ID} and k_{IM} are the nonradiative decay from the excimer and monomer, respectively. Figure 3 shows that no differences in excimer formation of DL- and L-A1PME are observed at room temperature.

In order to determine k_{DM}, k_{MD}, and k_D separately, fluorescence decay curves as a function of concentration are measured at room temperature. The decay curves in the excimer region (490 nm) can be fitted as a difference of two exponentials with λ_1 and λ_2 as decay parameters and a preexponential ratio $\simeq -1$ (Figure 4B), whereas a sum of two exponentials with the same λ_1 and λ_2 as decay parameters and A as preexponential ratio fits the decay observed in the emission of the locally excited state (Figure 4A); these results suggest that the intermolecular excimer formation

(26) Berlman, I. B. *Handbook of the Fluorescence Spectra of Aromatic Molecules*; Academic: New York, 1971.
(27) Tournon, J.; Kuntz, E.; El-Bayoumi, M. A. *Photochem. Photobiol.* **1972**, *16*, 425.
(28) Hara, K.; Ware, W. R. *Chem. Phys.* **1980**, *51*, 61.
(29) (a) Weast, R. C. *Handbook of Chemistry and Physics*; CRC: Cleveland, 1971. (b) Redpath, A. E.; Winnik, M. A. *J. Am. Chem. Soc.* **1982**, *104*, 5604. (c) Cuniberti, C.; Perico, A. *Ann. N. Y. Acad. Sci.* **1981**, *366*, 35.

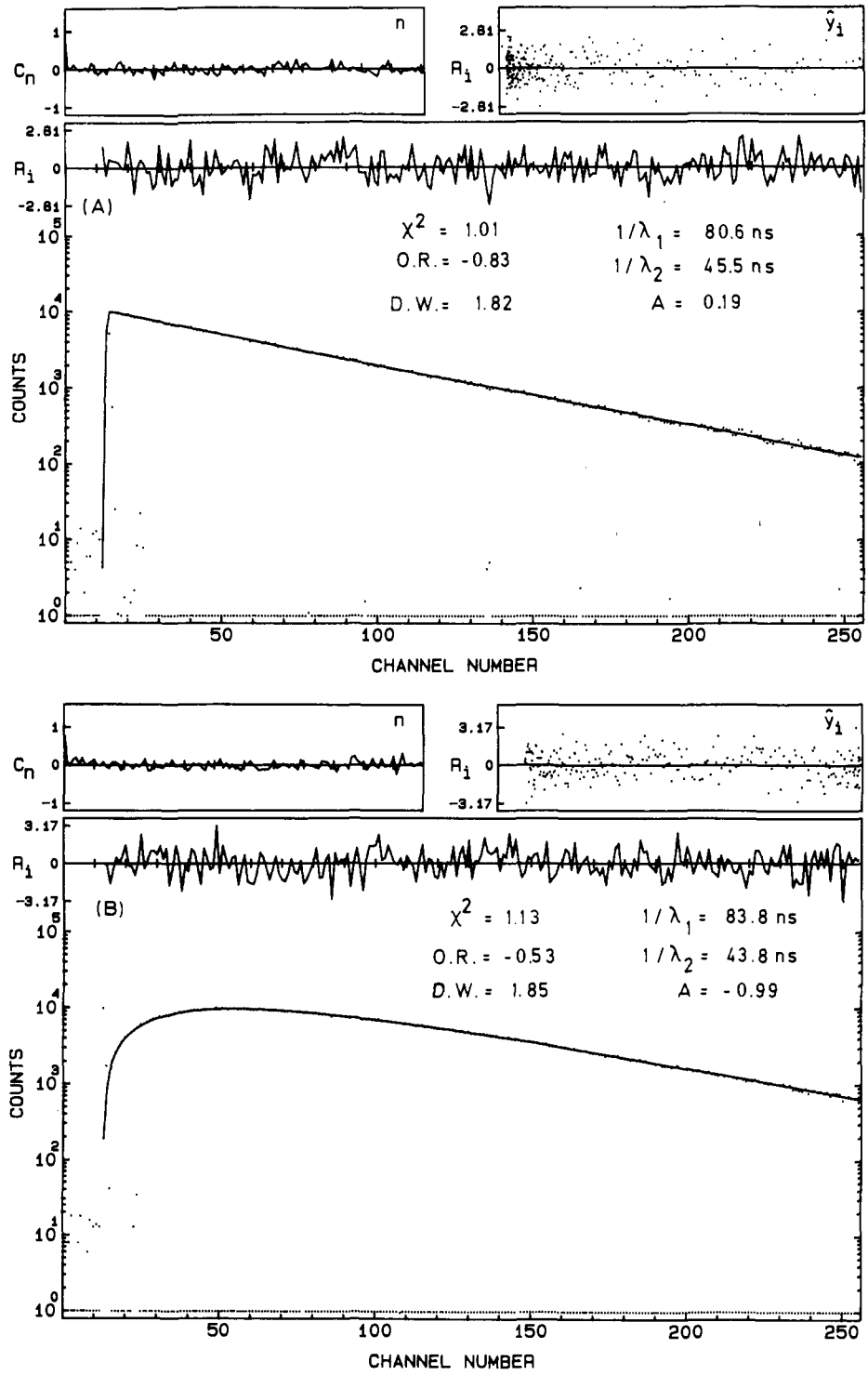

Figure 4. Fluorescence decay curves from the locally excited state (A) and the excimer emission region (B) of DL-A1PME in DMF (9.0×10^{-3} M) at room temperature, λ_{exc} = 340 nm (fitting and decay parameters within the figure).

of A1PME can be described adequately by the kinetic scheme presented above.[9] From the experimental decay parameters λ_1, λ_2, and A and the lifetime of A1PME in diluted solution ($\tau^\circ = 1/k_M$), $k_{DM}[M]$, k_{MD}, and k_D are calculated from eq 2, 3, and 4. The results obtained from eq 2 for DL- and L-A1PME in the three solvents studied are plotted vs. concentration in Figure 5, and the obtained linearity indicates that k_{DM} is concentration independent. Table I lists the rate constants obtained from fluorescence spectra and decay curves for DL- and L-A1PME at room temperature. The value of k_{DM} for DL-A1PME is somewhat smaller than for L-A1PME in inert solvents. This difference however lies within the experimental error, and it can be concluded that no important chiral discrimination affects the intermolecular excimer formation of A1PME at room temperature.

$$k_{DM}[M] = \frac{\lambda_1 + A\lambda_2}{A + 1} - k_M \quad (2)$$

$$k_{MD} = \frac{(k_{DM}[M] + k_M - \lambda_1)(\lambda_2 - k_{DM}[M] - k_M)}{k_{DM}[M]} \quad (3)$$

$$k_D = \lambda_1 + \lambda_2 - k_{DM}[M] - k_M - k_{MD} \quad (4)$$

The ratio of the k_{DM} values obtained in different solvents agrees with the inverse of the corresponding viscosity ratio. In the hydrogen-accepting solvent DMF, however, less excimer is observed than expected for solvent viscosity, even when the change of the lifetime of A1PME in diluted solution with the solvent is taken into account. The values of k_{DM} for pyrene in acetonitrile

Table I. Rate Constants Obtained from Decay Curves and Fluorescence Spectra of Racemic (DL-) and Optically Pure (L-) A1PME at Room Temperature[a]

	acetonitrile		toluene		DMF	
	DL-A1PME	L-A1PME	DL-A1PME	L-A1PME	DL-A1PME	L-A1PME
k_{DM}, M^{-1} s^{-1}	4.8 (±0.4) × 10^9	5.0 (±0.3) × 10^9	2.6 (±0.2) × 10^9	2.7 (±0.2) × 10^9	1.0 (±0.1) × 10^9	1.0 (±0.1) × 10^9
k_{MD}, s^{-1}	0.9 (±0.5) × 10^6	1.4 (±0.4) × 10^6	1.5 (±0.5) × 10^6	2.0 (±0.5) × 10^6	1.5 (±0.5) × 10^6	2.5 (±1.0) × 10^6
k_D, s^{-1}	1.8 (±0.2) × 10^7	1.7 (±0.1) × 10^7	1.9 (±0.1) × 10^7	1.9 (±0.1) × 10^7	1.9 (±0.1) × 10^7	1.8 (±0.2) × 10^7
K, M^{-1}	10.2 (±0.4) × 10^2	10.3 (±0.4) × 10^2	6.0 (±0.4) × 10^2	6.1 (±0.3) × 10^2	2.0 (±0.1) × 10^2	2.0 (±0.1) × 10^2
η, cps[29]	0.345	0.345	0.558	0.558	0.784	0.784

[a] Experimental errors in parentheses.

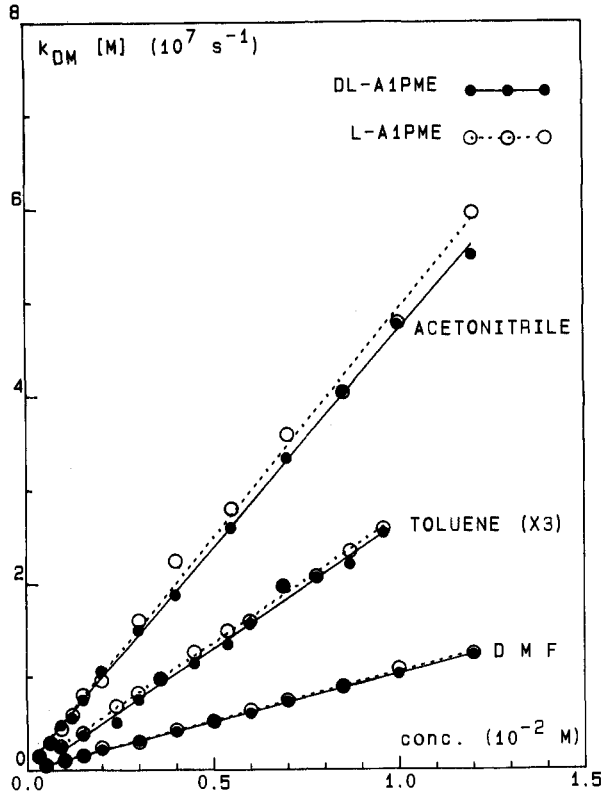

Figure 5. $k_{DM}[M]$ values obtained from fluorescence decay curves (eq 2) vs. the concentration at room temperature.

and toluene have been determined[30] and equal 1.2 × 10^{10} and 4.7 × 10^9 M^{-1} s^{-1}, respectively. This value is larger than that for A1PME, indicating a decrease of the efficiency of excimer formation per collision. This could be due to the bulkiness of the substituent of A1PME and would be even more important in DMF, where the peptide function is solvated, than in inert solvents.

Although no differences of the k_D values of the excimer formed in DL- and L-A1PME (Table I) are observed, a larger k_{MD} is calculated for L-A1PME at room temperature in the three solvents studied, suggesting a chiral discrimination in the dissociation from the excimer to the locally excited state. In addition, larger k_{MD} values are obtained in the more viscous DMF than in acetonitrile and toluene, indicating an enhanced stabilization of the excimer in inert solvents and/or a destabilization in the hydrogen-accepting solvent. This effect will be discussed in more detail below.

The difference in k_{MD} due to chiral discrimination and the absence of a difference in k_{DM} and k_D imply a chiral discrimination in the ϕ_D/ϕ_M values according to eq 1. However, k_{MD} is much smaller than k_D at room temperature, and the contribution of k_{MD} to $k_D + k_{MD}$ is not important. Therefore the chiral effect on k_{MD} is for the ratio ϕ_D/ϕ_M within the experimental error (Figure 3).

In order to determine the thermodynamic parameters of the process of intermolecular excimer formation in A1PME and to show that the D–L and the L–L excimer have a different stabili-

(30) Birks, J. B.; Dyson, D. J.; Munro, I. H. *Proc. R. Soc. London, A* **1963**, *275*, 575.

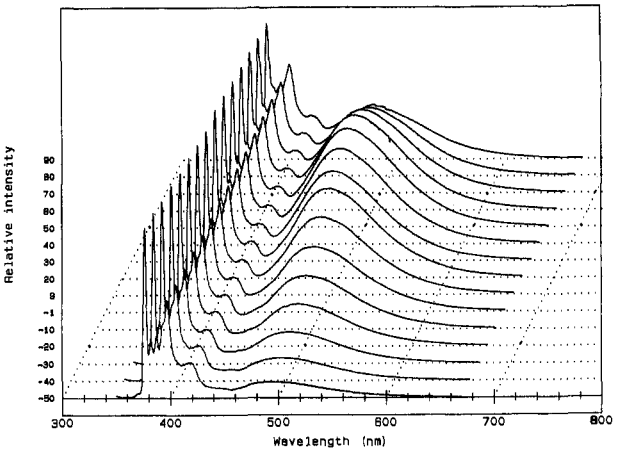

Figure 6. Fluorescence spectra of DL-A1PME (1.1 × 10^{-2} M) in DMF at different temperatures (left edge), λ_{exc} = 343 nm.

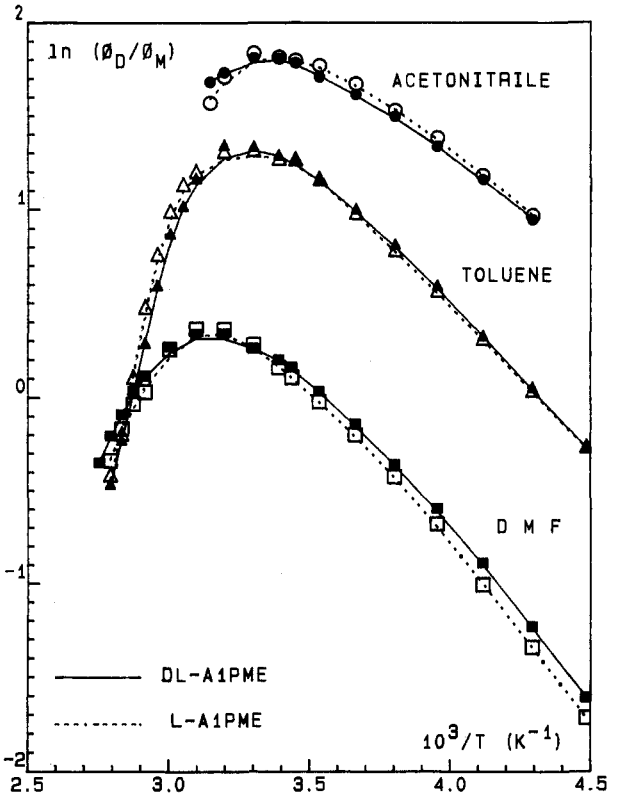

Figure 7. Average values of the natural logarithm of the ϕ_D/ϕ_M ratio vs. the inverse of the absolute temperature, [A1PME] = 6.0 × 10^{-3} M. In toluene, the results obtained at 2.0 × 10^{-3} M are extrapolated to 6.0 × 10^{-3} M.

zation, affected by the tendency of the solvent to interact by hydrogen bonding with the peptide function, fluorescence spectra and decays of DL- and L-A1PME at two concentrations (1.0 × 10^{-2} and 2.0 × 10^{-3} M) are measured as a function of temperature. Figure 6 shows the evolution of the fluorescence spectra with temperature, and in Figure 7 the natural logarithm of the ϕ_D/ϕ_M

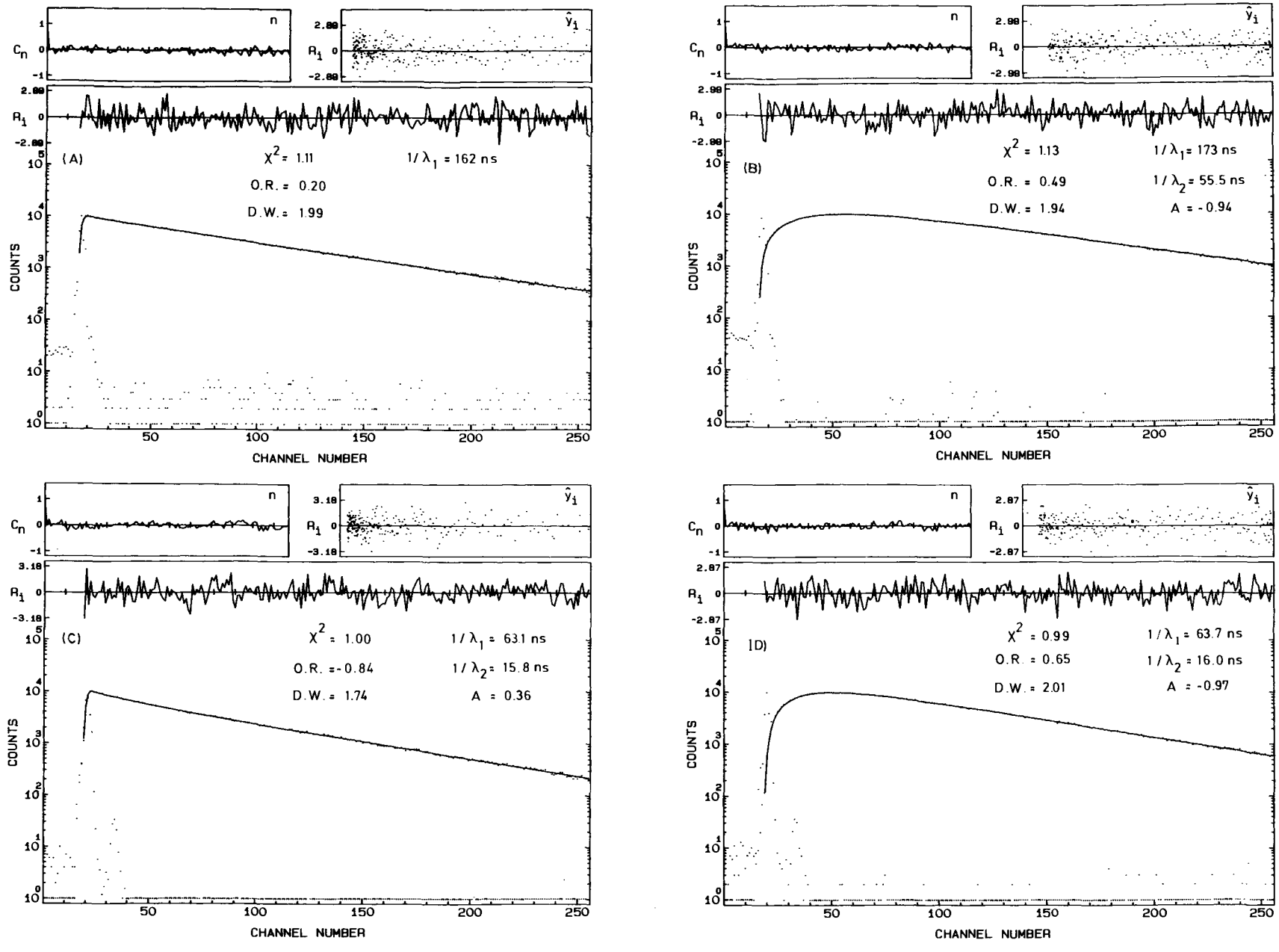

Figure 8. Fluorescence decay curves of DL-A1PME in DMF (9.2×10^{-3} M): at −40 °C, (A) λ_{em} = 378 nm and (B) λ_{em} = 490 nm; at 70 °C, (C) λ_{em} = 378 nm and (D) λ_{em} = 490 nm (fitting and decay parameters within the figure).

Table II. Thermodynamic Parameters for Racemic (DL-) and Optically Pure (L-) A1PME, Obtained from Arrhenius Plots [Figure 9: (a) Preexponential Constant, (b) Activation Energy], Activation Energy of Solvent Viscosity (E_η), and $E_{DM} - E_D$ from Fluorescence Spectra Measurements[a]

	acetonitrile		toluene		DMF	
	DL-A1PME	L-A1PME	DL-A1PME	L-A1PME	DL-A1PME	L-A1PME
k°_{DM},[c] M^{-1} s^{-1}	2.1×10^{11}	2.3×10^{11}	4.5×10^{11}	4.5×10^{11}	7.2×10^{11}	6.9×10^{11}
E_{DM},[d] kcal/mol	2.2 (± 0.1)	2.2 (± 0.1)	3.0 ± 0.1	3.0 ± 0.1	3.8 ± 0.1	3.8 ± 0.2
k°_{MD},[a] s^{-1}	4.5×10^{15}	8.0×10^{14}	3.3×10^{15}	1.4×10^{15}	3.0×10^{15}	7.3×10^{14}
E_{MD},[b] kcal/mol	13.2 (± 0.3)	11.8 (± 0.4)	12.6 ± 0.6	12.0 ± 0.5	12.6 ± 0.5	11.8 ± 0.6
ΔS°, cal/(K mol)	−20	−16	−18	−16	−17	−14
ΔH°, kcal/mol	−11.0	−9.6	−9.6	−9.1	−8.8	−8.0
ΔG°, kcal/mol[b]	−5.2	−4.9	−4.3	−4.4	−3.7	−3.9
$E_{DM}-E_D$, kcal/mol	2.3 (± 0.7)	2.3 (± 0.1)	3.1 ± 0.1	3.0 ± 0.1	3.8 ± 0.1	3.9 ± 0.1
E_η, kcal/mol[29]	1.7	1.7	2.2	2.2	3.2	3.2

[a] Experimental errors are in parentheses. [b] 20 °C. [c] Preexponential constant. [d] Activation energy.

ratio is plotted vs. the inverse of the absolute temperature $1/T$ (ϕ_D/ϕ_M values in acetonitrile at high temperatures are not enclosed in Figure 7 because they are not reproducible, probably due to the low boiling point of this solvent). In the "low-temperature region" (below 0 °C) the linearity of ln (ϕ_D/ϕ_M) vs. $1/T$ indicates that k_{MD} is negligible compared to k_D, as shown by the single-exponential decay of the locally excited state emission (Figure 8A) observed in this temperature region. From the slope, the activation energy of excimer formation (E_{DM}) minus the activation energy of the inherent decay of the excimer (E_D) is calculated (Table II). The fluorescence decay curves analyzed at high temperatures can be fitted to a sum of two exponentials for the locally excited state and to a difference of two exponentials in the excimer region with identical decay parameters (Figure 8C and 8D), indicating that k_D is not negligible with respect to k_{MD} (for example, $k_{MD} = 3.2\ 10^7\ s^{-1}$ and $k_D = 3.6 \times 10^7\ s^{-1}$ are calculated for DL-A1PME in acetonitrile at 80 °C).

The evolution of the k_D, k_{DM}, and k_{MD} values, obtained from time-correlated single-photon counting measurements, as a function of temperature is shown in Figure 9. A large deviation of the linearity is observed for ln k_D vs. $1/T$, which could be attributed to the change of the contribution of the radiative (k_{FD}) and nonradiative (k_{ID}) excimer decay processes with the temperature. Since the absolute quantum yield cannot be determined accurately in front-face experiments, the separate determination of k_{FD} and k_{ID} could not be realized. The fact that k_D is not negligible compared to k_{MD} and that k_D has an important activation energy at high temperatures imply an important contribution of k_D to the slope of the linear relation of ln (ϕ_D/ϕ_M) vs. $1/T$ at high temperatures (Figure 7). This explains the discrepancy of the ΔH° values calculated from the fluorescence decay measurements and the stationary experiments.

Good linearity is observed in the Arrhenius plot of k_{DM} and k_{MD} (Figure 9); the deviation observed in k_{MD} at 0 °C is attributed to the large experimental error on the preexponential ratio in the decay curves at this temperature (incipient excimer redissociation). Table II lists the thermodynamic parameters obtained from fluorescence spectra and decay curves for DL- and L-A1PME in the three solvents studied. A good relation between E_{DM} and the activation energy of the solvent viscosity (E_η) is obtained. Birks reported a E_{DM} of 3.0 kcal/mol for pyrene in toluene,[31] which agrees quite well with our values. Since both k°_{DM} and E_{DM} are similar for DL- and L-A1PME in the three solvents, it is concluded that no important chiral discrimination affects the intermolecular excimer formation of A1PME. However, large differences of k°_{MD}, E_{MD}, ΔS°, and ΔH° values of DL- and L-A1PME are observed, indicating an important chiral discrimination in the dissociation from the excimer to the locally excited state.

An average $\Delta H^\circ = -9$ kcal/mol for the intermolecular excimer of pyrene compounds has been reported[9,30,31] for a large variety of solvents. Consequently, the following remarks should be made with regard to the influence of the solvent and the chirality of the substituent on the excimer of A1PME (Table II). (a) In toluene, no important difference in the enthalpy change between DL- and L-A1PME, and between A1PME and pyrene, is observed. (b) In acetonitrile, a larger stabilization enthalpy and entropy loss are observed in the excimer formation of DL-A1PME compared to L-A1PME and also compared to those in toluene. (c) In DMF, a smaller stabilization enthalpy and entropy loss are obtained for L-A1PME compared to DL-A1PME and compared to those in toluene.

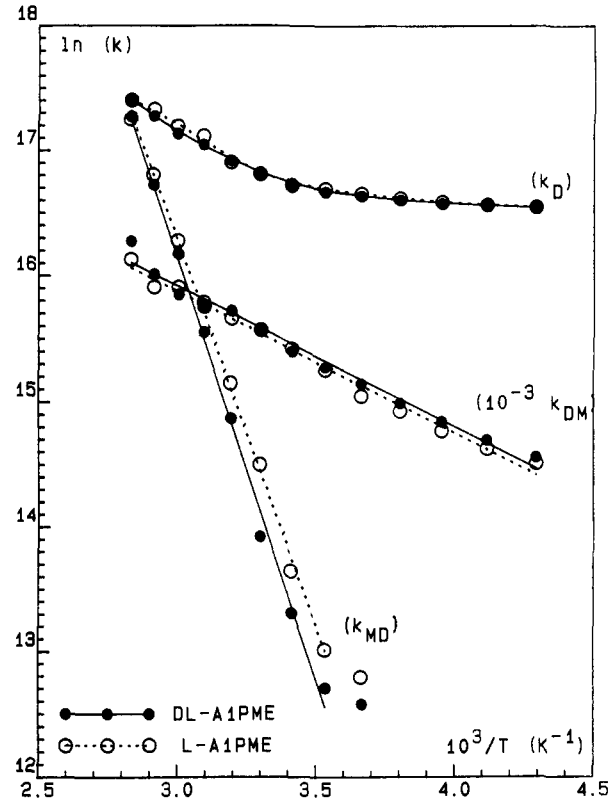

Figure 9. Arrhenius plot for the rate constants k_{DM}, k_{MD}, and k_D of A1PME in acetonitrile (average values obtained at 1.0×10^{-2} M and 2.0×10^{-3} M).

Discussion

A study of the intermolecular formation of L-A1PME in toluene and DMF by means of circularly polarized fluorescence spectroscopy has been reported[14]. After excitation at 280 nm, the dissymmetry factor in toluene has been observed to be independent of the emission wavelength in the excimer region, whereas in DMF a large wavelength dependence has been reported. From these results and taking into account the different polarity of the solvents, two types of excimer have been proposed: an apolar [Py*–Py ↔ Py–Py*] excimer and a [Py^+–Py^- ↔ Py^-–Py^+) excimer which is favored in polar media with a longer interchromophoric distance (shorter emission wavelength) than the nonpolar excimer. Since the full width at medium height of the excimer band of A1PME

(31) Sadovskii, N. A.; Shilling, R. D.; Kuzmin, M. G. *J. Photochem.* **1985**, *31*, 247.

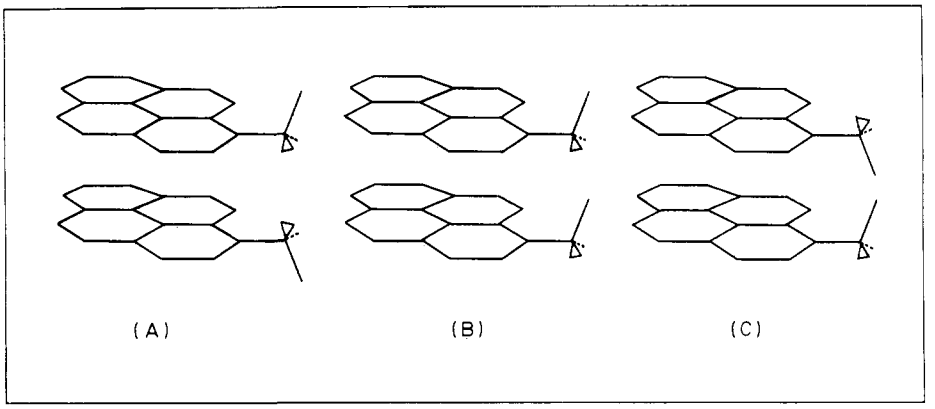

Figure 10. Different orientations of the substituent of A1PME in the geometry excimer.

is the same, within experimental error, in polar solvents (3500 cm^{-1} in acetonitrile and DMF) and an apolar medium (3400 cm^{-1} in toluene), no evidence of a second excimer is obtained in this contribution (the polar excimer has been estimated to fluoresce around 460 nm).[14] The existence of a second intermolecular excimer in A1PME is further checked by other methods: in transient fluorescence spectra no change of the excimer emission band at variable delay time after excitation is observed, and the decay parameters in the excimer region are independent of the analysis wavelength. Recently, ionic excited states of A1PME have been studied[32] by transient absorption spectroscopy using appropriate electron-transfer quenchers, and it could be concluded that ionic pyrene excited states are formed by a two-photon process via a Rydberg state. For pyrene, the energy of this Rydberg state is estimated at about 5 eV ($\simeq$250 nm) above the ground state, not so far from the excitation wavelength used by Egusa et al.[14] (280 nm). In the present contribution, the excitation wavelength is 343 nm, and the proposed formation of any ionic species from the Rydberg state can be neglected.

Changes in the dissymmetry factor with the emission wavelength in the excimer emission region of 1-(1-hydroxyhexyl)pyrene[13] have been reported in methanol, and this behavior has been attributed either to the presence of more than one emitting species with different chiroptical properties and to the emission of two different excited states.

In order to explain the solvent and the chiral effect on the stabilization of the excimer, different orientations of the substituent of A1PME in the excimer geometry are taken into account in Figure 10: in orientation (A) the peptide functions are far apart and low chiral discrimination is expected; in orientation (C) both peptide functions are very close and a large steric hindrance should result as concluded from molecular models; the orientation (B) seems to be the most important to contribute to the chiral discrimination as hydrogen bond interactions are possible between the amino acid chains. Hydrogen bond interactions between the NH amide group of one amino acid chain with the carboxyl function of the other could be possible in the heterotactic D–L (or L–D) excimer (Figure 11A), whereas in the homotactic L–L (or D–D) excimer no hydrogen bonding is possible (Figure 11B). In inert solvents as acetonitrile, this hydrogen bonding could stabilize the heterotactic D–L excimer with respect to the homotactic L–L excimer. A difference of 1.5 kcal/mol on the stabilization enthalpy $\Delta H°$ is obtained between DL- and L-A1PME in acetonitrile; of course, DL-A1PME can form both the homotactic L–L (or D–D) excimer and the heterotactic D–L (or L–D) excimer with about the same probability because no important chiral discrimination is observed in the rate constant of the excimer formation process, implying a stabilization of 3 kcal/mol in the D–L excimer with respect to the L–L excimer. Table II shows that the preexponential constant $k°_{MD}$ of DL-A1PME is larger than that of L-A1PME, resulting in an inversion of the k_{MD} values at high temperatures compared to those at room temperature (Table I). This inversion

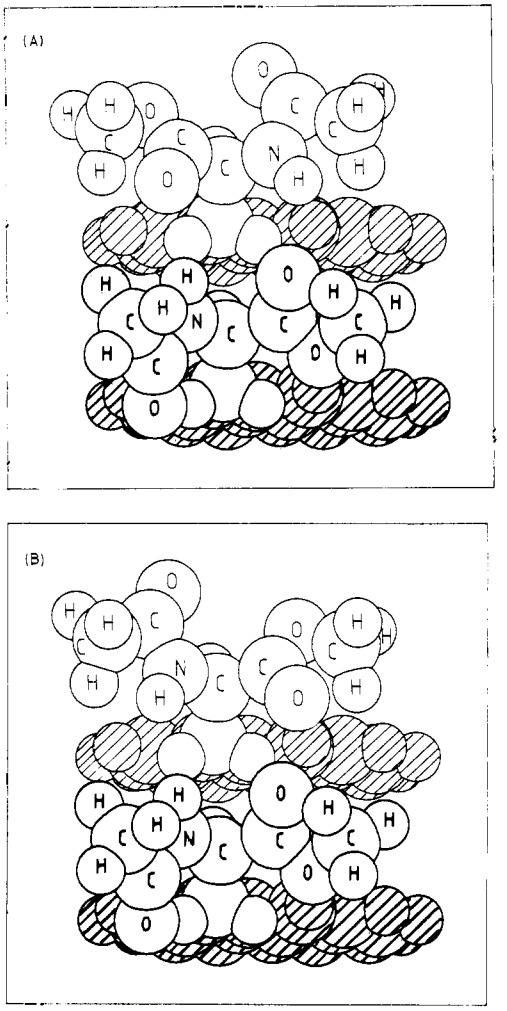

Figure 11. Conformational plots of (A) D–L excimer (B) L–L excimer of A1PMe. Pyrene chromophores are shaded.

can be explained by considering the influence of the entropy change. The additional hydrogen bonding which stabilizes the D–L excimer implies a higher arrangement of the molecules in this excimer, and therefore the D–L excimer has a lower entropy change than the L–L excimer (Table II). The contribution of $\Delta S°$ in $\Delta G°$ is more important at higher temperatures where the larger enthalpic stabilization of the D–L excimer could be compensated by its unfavored entropy. In hydrogen-accepting solvents as DMF, the NH amide groups are solvated, increasing the bulkiness of the substituent in A1PME. Consequently, the steric hindrance between the substituents could destabilize the excimer interaction, which should be more important in the L–L excimer (the two amide groups are opposite one another, Figure 11B) than in the D–L excimer.

(32) Masuhara, H.; Tanaka, J.; Mataga, N.; Sisido, M.; Egusa, S.; Imanishi, Y. *J. Phys. Chem.* **1986**, *90*, 2791.

Conclusion

The emission of only one excimer in the spectrum of A1PME is confirmed by the independence of the thermodynamic parameters of the excimer-monomer equilibrium with solvent polarity.

Although no important chiral discrimination is observed in the excimer formation process of A1PME in the three solvents studied, two chiroptical excimers, the homotactic L-L and the heterotactic D-L pairs, are formed with a different stabilization, resulting in a different rate constant for the dissociation from the excimer to the locally excited state.

The additional stabilization of the D-L excimer in inert solvents is ascribed to a hydrogen bond interaction between the amino acid chains in the excimer geometry, which is more likely in the heterotactic excimer. Because the chiral discrimination is observed in the excimer dissociation and not in the excimer formation process and because no intermolecular hydrogen bonding in the ground state of A1PME is observed by infrared spectroscopy, the additional stabilization of the D-L excimer is obtained by hydrogen bond interaction between the amino acid chains after the excimer geometry is adopted by the chromophores. A similar conclusion was obtained by Lapp and Laustriat[33] to explain the smaller rate constant of the excimer dissociation process in 3-phenylpropamide compared to phenylethane in dichloroethane.

Acknowledgment. We are indebted to the F.K.F.O. for financial assistance to the laboratory. The Basque Country Government and the N.F.W.O. are thanked, the former for a fellowship to F.L.-A. and the latter for a fellowship to R.G. and F.R.

(33) Lapp, C. F.; Laustriat, G. *J. Chim. Phys.* **1971**, *68*, 159.

Covalent Electrophilic Catalysis of the Breakdown of Hyponitrite to Nitrous Oxide by Aldehydes, Ketones, and Carbon Dioxide[1a]

Edward L. Loechler,*[1b] Andrew M. Schneider,[1c] David B. Schwartz,[1c] and Thomas C. Hollocher*[1c]

Contribution from the Department of Biology, Boston University, Boston, Massachusetts 02215, and the Department of Biochemistry, Brandeis University, Waltham, Massachusetts 02254.
Received June 30, 1986

Abstract: Catalysis of the breakdown of *trans*-hyponitrite monoanion ($HN_2O_2^-$) into N_2O by aldehydes and ketones was studied spectrophotometrically in aqueous solution from pH 6 to 12.5 at 25 °C, ionic strength 1.0 M (KCl), and that of *trans*-hyponitrite dianion by CO_2 was studied similarly from pH 7 to 12.5. The reactions are first order with respect to hyponitrite and catalyst concentrations. Only the monoanion reaction is observed with aldehydes and ketones and only the dianion reaction with CO_2. The species active in catalysis are shown to be unhydrated carbonyl and CO_2. The correlation between the logarithm of the second-order catalytic rate constant and the Taft σ^* values for substituents at the carbonyl carbon is linear with $\rho^* = 1.80$ and 1.68 for free aldehydes and ketones, respectively. For carbonyl hydration, $\rho^* = 1.68$ and for ionization of the hydrates, 1.40. Kinetic arguments support mechanisms (Scheme III) in which *trans*-hyponitrite forms a nitrogen adduct with a carbonyl or CO_2, after which the adduct experiences rate-determining isomerization to its cis isomer. This form of the adduct then reverts to catalyst and *cis*-hyponitrite, which rapidly breaks down to N_2O. The breakdown of *cis*-hyponitrite involves trans periplanar elimination of hydroxide ion, and this probably accounts for its greater instability relative to *trans*-hyponitrite. Isomerization requires inversion or rotation at a N,N-double bonded nitrogen in *trans*-hyponitrite, and the adducts catalyze isomerization by stabilizing resonance forms with N,N-single bond character. These reactions appear to be examples of covalent electrophilic catalysis. Arguments are presented which suggest that the uncatalyzed breakdown of hyponitrite proceeds by a similar mechanism involving protonation of nitrogen and rate-determining isomerization.

The monomolecular breakdown of hyponitrite (HO-N=N-OH, *trans*- (*anti*- or *E*)-hyponitrous acid) to N_2O in aqueous solution proceeds by way of a monoanionic species above pH 3 and an uncharged species between pH 0 and 3.[2-4] In the H_0 range of acidities, acid catalysis is observed.[2,4] These reactions appear not to be radical chain reactions,[2,4] and the N_2O is produced without N-N bond cleavage.[5] A solvent isotope effect, k_H/k_D, of 1.3 was reported for the monoanion reaction at pH 8.5, 1.95 for the neutral reaction at pH 1 and 1.43-1.50 in sulfuric acid solutions.[2] ΔS^* is small for the monoanion (6 ± 5 eu) and neutral (-5.8 ± 0.7 eu) reactions and -18 to -30 eu for the acid-catalyzed reactions.[2] These data, plus ionic strength effects associated particularly with the monoanion reaction, led Buchholz and Powell[2] to postulate direct expulsion of hydroxide ion from *trans*-hyponitrite monoanion, rate-determining intramolecular proton transfer within neutral *cis*-hyponitrite, and rate-determining intermolecular proton transfer in the acid-catalyzed reactions. We find little in the data to support these mechanisms convincingly and suggest that the mechanisms of hyponitrite breakdown are poorly understood.

An alternative mechanistic possibility[4] is one in which the rate-determining step is the isomerization of *trans*-hyponitrite or its conjugate acids to putative *cis*-hyponitrite, which is probably very unstable. The basis of this possibility is the observation by Hussain et al.[6] that N_2O and *trans*-hyponitrite can be produced simultaneously in the reaction between HNO_2 and NH_2OH and that the N_2O is produced via a symmetrical dinitrogen precursor, which is probably *cis*-hyponitrous acid.[6,7] In that reaction, the

(1) (a) Supported by grants from the National Science Foundation (PCM 79-12566 and PCM 82-18000) and Biomedical Research Support Grant S07 RR07044 from the National Institutes of Health. (b) Boston University. (c) Brandeis University.

(2) Buchholz, J. R.; Powell, R. E. *J. Am. Chem. Soc.* **1963**, *85*, 509-511.

(3) Hughes, M. N.; Stedman, G. *J. Chem. Soc.* **1963**, 1239-1243.

(4) Hughes, M. N.; Stedman, G. *J. Chem. Soc.* **1964**, 163-166.

(5) Aktar, M. J.; Balschi, J. A.; Bonner, F. T. *Inorg. Chem.* **1982**, *21*, 2216-2218.

(6) Hussain, M. A.; Stedman, G.; Hughes, M. N. *J. Chem. Soc. B* **1968**, 597-603.

(7) Bonner, F. T.; Kada, J.; Phelan, K. G. *Inorg. Chem.* **1983**, *22*, 1389-1391.

0002-7863/87/1509-3076$01.50/0